Photoproduction of Proton Gradients with π-Stacked Fluorophore Scaffolds in Lipid Bilayers

Sheshanath Bhosale,[1] Adam L. Sisson,[1] Pinaki Talukdar,[1] Alexandre Fürstenberg,[2] Natalie Banerji,[2] Eric Vauthey,[2] Guillaume Bollot,[1] Jiri Mareda,[1] Cornelia Röger,[3] Frank Würthner,[3] Naomi Sakai,[1] Stefan Matile[1]*

Rigid *p*-octiphenyl rods were used to create helical tetrameric π-stacks of blue, red-fluorescent naphthalene diimides that can span lipid bilayer membranes. In lipid vesicles containing quinone as electron acceptors and surrounded by ethylenediaminetetraacetic acid as hole acceptors, transmembrane proton gradients arose through quinone reduction upon excitation with visible light. Quantitative ultrafast and relatively long-lived charge separation was confirmed as the origin of photosynthetic activity by femtosecond fluorescence and transient absorption spectroscopy. Supramolecular self-organization was essential in that photoactivity was lost upon rod shortening (from *p*-octiphenyl to biphenyl) and chromophore expansion (from naphthalene diimide to perylene diimide). Ligand intercalation transformed the photoactive scaffolds into ion channels.

In biological systems, light harvesting uses the energy in photons to drive chemical reactions. Although many biomimetic and supramolecular compounds have been devised to collect photons, the output of these systems often consists of photons of lower energy. The outstanding challenge is to devise schemes in which acceptor chromophores can transfer the charge carrier (electron or hole) to generate a chemical product (for example, H^+ or O_2) before relaxation to the initial state occurs.

In proteins, a series of chromophores is used to separate charges and avoid back reactions (*1–3*). In smaller biomimetic assemblies, an alternative strategy is to transfer charge to electron donors and acceptors in solution, provided that these donors and acceptors can be spatially separated and that these transfers occur faster than the charge recombination (*4–7*). We report the design, synthesis, and evaluation of blue, red-fluorescent rigid-rod photosystems (**1**), in which the π-stack apparently supports sufficient charge-separation lifetimes for conversion into chemical gradients (Fig. 1).

The construction of complex and multifunctional π-architecture is difficult because of the poor directionality of π,π-interactions (*8–18*). Apart from a central role in oligonucleotide chemistry and biology (*18*), cofacial π-stack architecture contributes very little to electron transfer in biological (*1–3*) and synthetic (*4–7*) photosystems, not to speak of the structure of biological or synthetic ion channels or pores (*19*). Recently, we have demonstrated that the rational design of refined transmembrane π-stack architecture is feasible with the use of rigid-rod molecules as preorganizing scaffolds (*20, 21*). This strategy was applied not only to create photosystem **1** but also to introduce multifunctionality; that is, to enable photosystem **1** to open up into ion channel **2** in response to the intercalation of ligands **3** (Fig. 1).

Photosystem **1** was prepared by self-assembly of four *p*-octiphenyls (**4**), each bearing eight core-substituted naphthalene diimides (NDIs) (*22*) along the rigid-rod scaffold (Fig. 2 and scheme S1). The NDI octamer **4** was synthesized from simple commercial starting materials **5** to **10** in 20 steps altogether. Pyrene **5** was oxidized to the core-chlorinated dianhydride to allow for the introduction of terminal (**6** and **7**) and central (**8**) amines before attachment along the *p*-octiphenyl rod made from four biphenyls (**10**) (*23*). The following control molecules were synthesized in a similar manner: NDI dimer **11**, NDI monomer **12**, perylene diimide (PDI) octamer **13**, and PDI dimer **14** (schemes S2 and S3).

Unsubstituted NDIs are colorless nonfluorescent electron traps. However, recent findings show that a minor change on the structural level suffices to introduce all of the characteristics needed for photosynthetic activity. Core substitution with electron-donating alkylamines produces compact blue, red-emitting push-pull fluorophores (excitation wavelength λ_{ex} = 638 nm; emission wavelength λ_{em} = 678 nm), lowers the reduction potential by 300 mV, and moves the oxidation potential within reach (*22*). The resulting potentials for NDI reduction to the radical anion $NDI^{\cdot-}$ [redox potential ($E_{1/2}$) = –710 mV] and oxidation to $NDI^{\cdot+}$ ($E_{1/2}$ = +1290 mV) appeared compatible with photoinduced charge separation in π-stack architecture **1** for electron transfer to
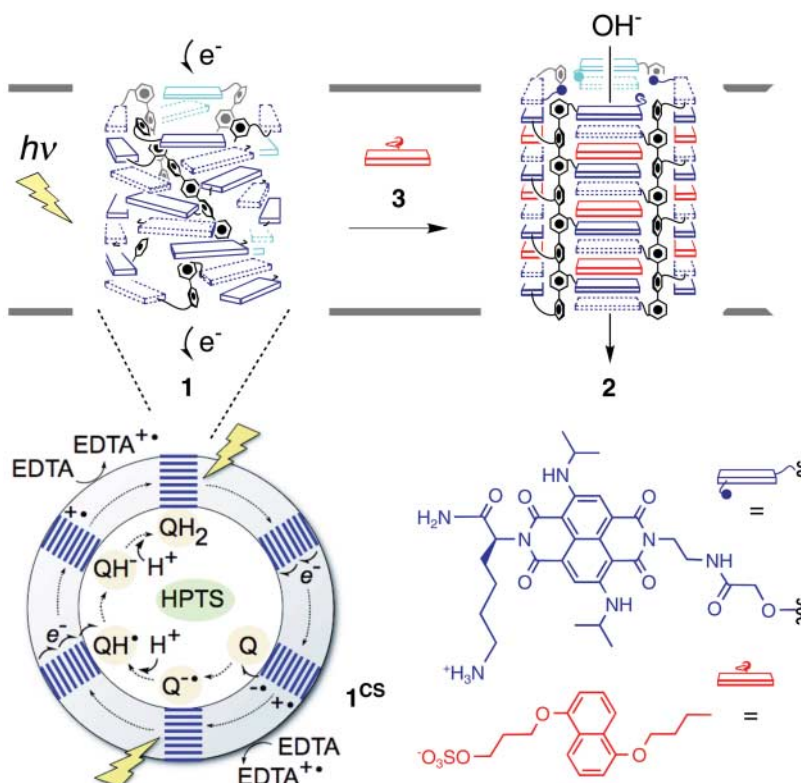
[1]Department of Organic Chemistry, [2]Department of Physical Chemistry, University of Geneva, Geneva, Switzerland. [3]Institut für Organische Chemie, Universität Würzburg, Am Hubland, D-97074 Würzburg, Germany.

*To whom correspondence should be addressed. E-mail: stefan.matile@chiorg.unige.ch

Fig. 1. Smart photosystem **1** with an indication of the ligand-gated opening into ion channel **2** and fluorometric detection of photosynthetic activity in bilayer membranes with HPTS as internal increase in pH after photoinduced charge separation (**1**^{CS}), followed by external EDTA oxidation and internal reduction of quinones (Q). *hv*, photonic energy.

2-sulfonato-1,4-naphthoquinone (Q) ($E_{1/2}$ = –60 mV) and hole transfer to EDTA ($E_{1/2} \approx$ +430 mV) (table S1). This photoredox process is thermodynamically unfavorable and thus converts photonic energy into chemical energy.

The photosynthetic activity of quadruple π-M-helices **1** was measured in egg yolk phosphatidylcholine large unilamellar vesicles (EYPC LUVs). The vesicles were loaded with quinone acceptor Q and pH detector 8-hydroxypyrene-1,3,6-trisulfonate (HPTS) and surrounded with the electron donor EDTA (Fig. 1) (4, 20). Internal quinone reduction in response to the irradiation of the externally added NDI rods **4** at 635 nm was detectable as an increase in intravesicular pH ("a" in Fig. 3A and fig. S4). The initial velocity of change in HPTS emission,

which reflects internal proton consumption, was analyzed with Hill's equation. The value of *n* = 3.9 ± 1.2 that was found indicated that the active photosystem **1** is a tetrameric supramolecule with a median effective concentration of 1.3 μM (Fig. 3B) (24). Judged from exciton coupling between twisted proximal NDI chromophores throughout circular dichroism (CD) spectra (21), this tetramer is a heat-insensitive (melting temperature ≥ 70°C) M-helix with sensitivity toward chemical denaturation [with guanidinium chloride, free energy of self-organization (ΔG^{H2O}) ≤ 1.17 kcal/mol, fig. S7]. Support for cofacial π-stacking (8) in quadruple π-M-helix **1** was secured with the appearance of a hypsochromic maximum at 598 nm that was absent in the absorption spec-

trum of monomer **12** and was much weaker with dimer **11** (fig. S9).

Time-resolved fluorescence and transient absorption measurements provided direct experimental evidence that, upon irradiation of **4**, a charge-separated state characterized by a relatively long lifetime (61 ps with **4** versus 23 ps with **11**) is populated almost quantitatively (>97%, compared to 68% with **11**) on an ultrafast time scale (with a distribution of time constants between <2 and ~7 ps) (Fig. 4 and figs. S12 to S17). These features account for the marked activity of photosystem **1**. The appearance of new bands in the transient absorption spectrum of the NDI monomer **12** (trace a in Fig. 4) in the presence of the electron donor *N,N*-dimethylaniline (DMA) confirmed that the radical anion NDI·⁻ was being detected (trace b in Fig. 4). The presence of the NDI·⁻ bands in the transient absorption spectra of dimer **11**, as well as bands of the more pronounced, more stable octamer **4**, supported photoinduced population of charge-separated state $\mathbf{1}^{CS}$ (trace c in Fig. 4).

The addition of intercalator **3** caused a ligand-gated helix-barrel transition from photosystem **1** to ion channel **2** (fig. S5) (20, 21) and thus resulted in the deletion of light-induced proton gradients [Figs. 1 and 3A (parts a and b)]; addition of the ion channel gramicidin A caused the same result. Photosynthetic activity was naturally inhibited by intercalator **3** (part d in Fig. 3A). The helix-barrel transition by intercalator **3** was also reflected in the expected CD silencing (21, 25), together with a small increase in emission intensity that may be interpreted as hindered charge separation in barrel-stave complex **2** (figs. S6 and S8).

Control molecules **11**, **13**, and **14** were made to elucidate the dependence of photosynthetic activity of photosystem **1** on rod contraction from *p*-octiphenyl to biphenyl and on chromophore expansion from NDI to PDI. Inactivity of NDI dimer **11** (part c in Fig. 3A) coincided with CD silencing, the partial disappearance of the 598-nm absorption indicative of cofacial π-stacking, and incomplete photoinduced charge separation with a reduced lifetime (Fig. 4 and figs. S9 to S17). Notably, in contrast, the independence of both chiroptical and poor photosynthetic activity on rod length was found for the PDI series represented by octamer **13** and dimer **14** (fig. S20 and table S4). In agreement with molecular models (Fig. 5 and figs. S18 and S19), these results confirmed that the smart rigid-rod π-stack NDI nanoarchitecture of photosystem **1** is distinctive (that is, incompatible with the PDI series) and essential for function.
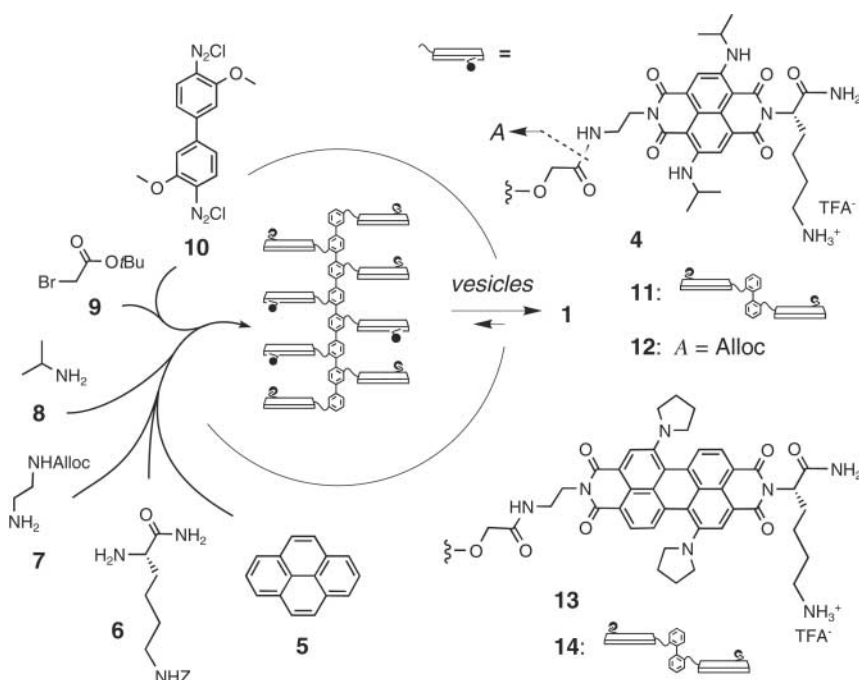

Fig. 2. Synthesis of rod **4** for self-assembly into photosystem **1** in lipid bilayers (Fig. 1) and structure of control molecules **11** to **14**.

Fig. 3. Photoactivity of NDI octamer **4** (a, solid circles) with in situ opening into ion channel **2** by addition of ligand **3** (b, open squares), and comparison to NDI dimer **11** (c, open circles) and preformed ion channel **2** (**4**+**3**, d,×). (**A**) Change in HPTS excitation ratio I_{462}/I_{405} (λ_{em} = 510 nm) as a function of irradiation time *t* (λ_{ex} = 635 nm) in the presence of **11** (10 μM) or **4** (1.5 μM) in EYPC LUVs (~65 μM) with external EDTA (5 mM; 0.95 mM $K_nH_{3-n}PO_4$, 95 mM KCl, pH 7.0) and internal quinone (10 mM) and HPTS (1 mM; 100 mM KCl, pH 7.0); ligand **3** (20 μM, or gramicidin A) was added at *t* = 10 min or *t* = 0 min. (**B**) Initial velocity of proton consumption as a function of the concentration c of **4** (solid circles) and **11** (open circles). Error bars indicate SE.
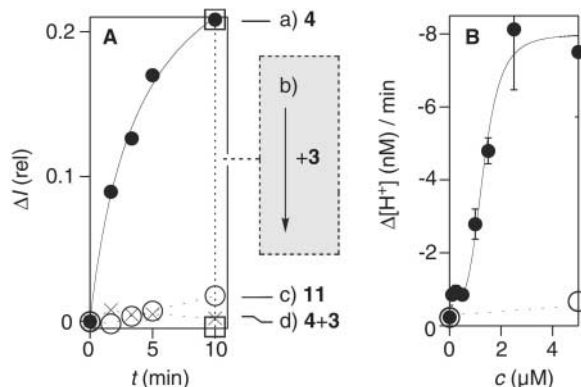
References and Notes

1. J. Deisenhofer, H. Michel, *Science* **245**, 1463 (1989).
2. P. Jordan *et al.*, *Nature* **411**, 909 (2001).
3. N. Nelson, A. Ben-Shem, *Nat. Rev. Mol. Cell Biol.* **5**, 971 (2004).

Fig. 4. Intensity-normalized transient absorption spectra of NDI octamer **4** (trace c) and NDI monomer **12** in the presence (trace b) or absence (trace a) of DMA in methanol after excitation with a 50-fs laser pulse at 600 nm. Δ absorbance, change in absorbance; a.u., arbitrary units. The bands at 510 and above 670 nm seen with **4** and **12** in the presence of DMA are attributed to the NDI$^{•-}$ radical, whereas with **12** in the absence of DMA, the 450- to 580-nm band originates from singlet excited-state absorption. The negative signal between 600 and 670 nm is due to ground-state bleaching and stimulated emission. (**Inset**) Time profiles of the absorption due to the radical anion of octamer **4** (circles) and dimer **11** ($\times$). The lines represent best fits to the data.
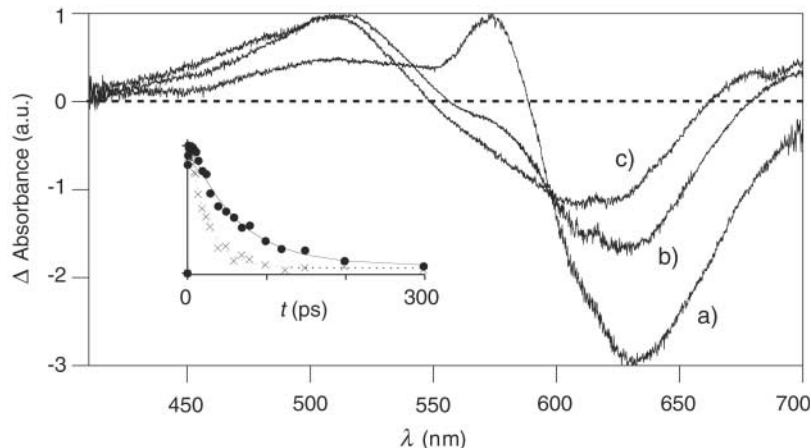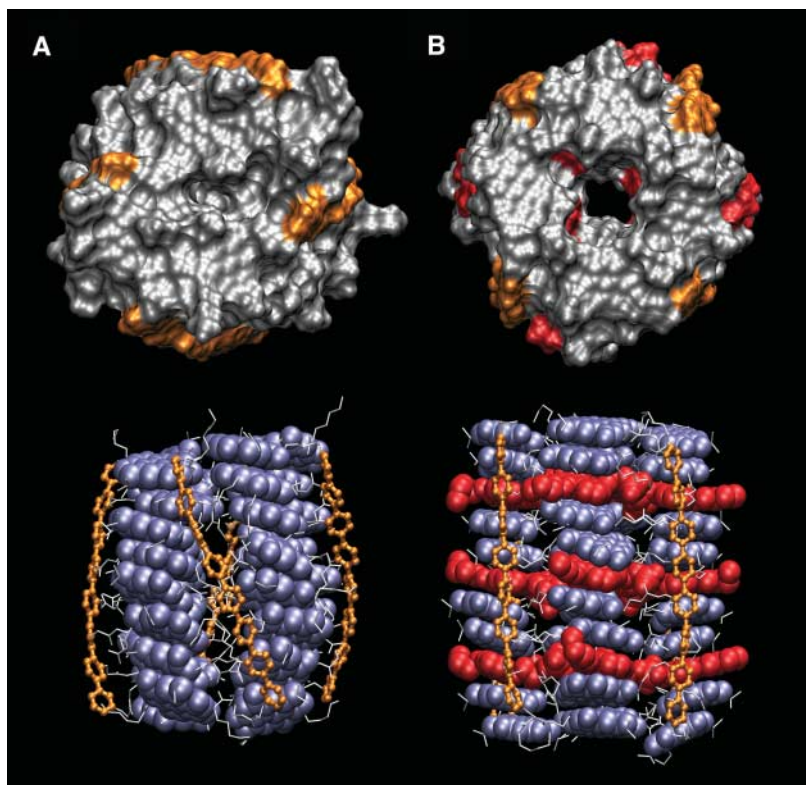

Fig. 5. Molecular dynamics simulations of photosystem **1** (**A**) and ion channel **2** (**B**) with 12 ligands **3** (red) in axial view (top) and side view (bottom). In (A) (closed pore), helicity (M) = $-50.2°$ and height (h) = 32 Å; in (B), inner diameter = 4.8 Å, $M = -8.8°$, and $h \approx 40$ Å.

4. G. Steinberg-Yfrach *et al.*, *Nature* **385**, 239 (1997).
5. J. J. Grimaldi, S. Boileau, J.-M. Lehn, *Nature* **265**, 229 (1977).
6. J. N. Robinson, D. J. Cole-Hamilton, *Chem. Soc. Rev.* **20**, 49 (1991).
7. L. Zhu, R. F. Khairutdinov, J. L. Cape, J. K. Hurst, *J. Am. Chem. Soc.* **128**, 825 (2006).
8. P. Giaimo, A. V. Gusev, M. R. Wasielewski, *J. Am. Chem. Soc.* **124**, 8530 (2002).
9. M. J. Ahrens *et al.*, *J. Am. Chem. Soc.* **126**, 8284 (2004).
10. L. L. Miller, K. R. Mann, *Acc. Chem. Res.* **29**, 417 (1996).
11. H. E. Katz *et al.*, *Nature* **404**, 478 (2000).
12. J. M. Warman *et al.*, *Chem. Mater.* **16**, 4600 (2004).
13. F. J. M. Hoeben, P. Jonkheijm, E. W. Meijer, A. P. H. J. Schenning, *Chem. Rev.* **105**, 1491 (2005).
14. V. Balzani, M. Venturi, A. Credi, *Molecular Devices and Machines* (Wiley, Weinheim, Germany, 2003), chap. 6.
15. L. Schmidt-Mende *et al.*, *Science* **293**, 1119 (2001).

16. R. S. Lokey, B. L. Iverson, *Nature* **375**, 303 (1995).
17. F. Würthner, Ed., *Supramolecular Dye Chemistry* (Topics in Current Chemistry Series **258**, Springer, Berlin, 2005).
18. C. Wan, T. Fiebig, O. Schiemann, J. K. Barton, A. H. Zewail, *Proc. Natl. Acad. Sci. U.S.A.* **97**, 14052 (2000).
19. S. Matile, A. Som, N. Sordé, *Tetrahedron* **60**, 6405 (2004).
20. P. Talukdar, G. Bollot, J. Mareda, N. Sakai, S. Matile, *J. Am. Chem. Soc.* **127**, 6528 (2005).
21. P. Talukdar, G. Bollot, J. Mareda, N. Sakai, S. Matile, *Chem. Eur. J.* **11**, 6525 (2005).
22. F. Würthner, S. Ahmed, C. Thalacker, T. Debaerdemaeker, *Chem. Eur. J.* **8**, 4742 (2002).
23. See supporting material on *Science* Online.
24. To confirm the validity of this result on the structural level, a CD method for the determination of meaningful Hill coefficients for exergonic self-assembly under denaturing conditions was introduced (*26*).
25. J. M. Kerckhoffs *et al.*, *J. Am. Chem. Soc.* **127**, 12697 (2005).

26. S. Bhosale, S. Matile, *Chirality*, in press.